MolecularMedicine

Regulation of Vascular Tone, Angiogenesis and Cellular Bioenergetics by the 3-Mercaptopyruvate Sulfurtransferase/H_2S Pathway: Functional Impairment by Hyperglycemia and Restoration by DL-α-Lipoic Acid

Ciro Coletta,[1] Katalin Módis,[1] Bartosz Szczesny,[1] Attila Brunyánszki,[1] Gábor Oláh,[1] Ester CS Rios,[1] Kazunori Yanagi,[1] Akbar Ahmad,[1] Andreas Papapetropoulos,[2] and Csaba Szabo[1]*

[1]Department of Anesthesiology, University of Texas Medical Branch, Galveston, Texas, United States of America; and [2]Faculty of Pharmacy, University of Athens, Greece; and *current affiliation: Cardiovascular and Metabolic Research Unit, Lakehead University, Thunder Bay, Ontario, Canada

Hydrogen sulfide (H_2S), as a reducing agent and an antioxidant molecule, exerts protective effects against hyperglycemic stress in the vascular endothelium. The mitochondrial enzyme 3-mercaptopyruvate sulfurtransferase (3-MST) is an important biological source of H_2S. We have recently demonstrated that 3-MST activity is inhibited by oxidative stress *in vitro* and speculated that this may have an adverse effect on cellular homeostasis. In the current study, given the importance of H_2S as a vasorelaxant, angiogenesis stimulator and cellular bioenergetic mediator, we first determined whether the 3-MST/H_2S system plays a physiological regulatory role in endothelial cells. Next, we tested whether a dysfunction of this pathway develops during the development of hyperglycemia and diabetes-associated vascular complications. Intraperitoneal (IP) 3-MP (1 mg/kg) raised plasma H_2S levels in rats. 3-MP (10 μmol/L to 1 mmol/L) promoted angiogenesis *in vitro* in bEnd3 microvascular endothelial cells and *in vivo* in a Matrigel assay in mice (0.3–1 mg/kg). *In vitro* studies with bEnd3 cell homogenates demonstrated that the 3-MP-induced increases in H_2S production depended on enzymatic activity, although at higher concentrations (1–3 mmol/L) there was also evidence for an additional nonenzymatic H_2S production by 3-MP. *In vivo*, 3-MP facilitated wound healing in rats, induced the relaxation of dermal microvessels and increased mitochondrial bioenergetic function. *In vitro* hyperglycemia or *in vivo* streptozotocin diabetes impaired angiogenesis, attenuated mitochondrial function and delayed wound healing; all of these responses were associated with an impairment of the proangiogenic and bioenergetic effects of 3-MP. The antioxidants DL-α-lipoic acid (LA) *in vivo*, or dihydrolipoic acid (DHLA) *in vitro* restored the ability of 3-MP to stimulate angiogenesis, cellular bioenergetics and wound healing in hyperglycemia and diabetes. We conclude that diabetes leads to an impairment of the 3-MST/H_2S pathway, and speculate that this may contribute to the pathogenesis of hyperglycemic endothelial cell dysfunction. We also suggest that therapy with H_2S donors, or treatment with the combination of 3-MP and lipoic acid may be beneficial in improving angiogenesis and bioenergetics in hyperglycemia.

Online address: http://www.molmed.org
doi: 10.2119/molmed.2015.00035

INTRODUCTION

Recent studies have demonstrated that the endogenous biological mediator hydrogen sulfide (H_2S) acts as a reducing agent and an antioxidant molecule (1–7). It exerts protective effects against hyperglycemic stress in the vascular endothelium and exhibits protective effects in animal models of diabetic complications (8–16).

The mitochondrial enzyme 3-mercaptopyruvate sulfurtransferase (3-MST) is a newly identified endogenous source of hydrogen sulfide (H_2S) in various cells and tissues, including vascular endothelial cells (17–19). We have recently demonstrated that 3-MST activity is inhibited by oxidative stress *in vitro* and speculated that this may exert adverse effects on cellular homeostasis (20,21). Given the importance of H_2S as a vasorelaxant (22–29), proangiogenic agent (27,30–36) and mitochondrial/bioenergetic modulator (20,21,35,37–42), here we examined whether the 3-MST/H_2S system plays physiological regulatory roles in endothelial cells. Next, we examined whether a dysfunction of the 3-MST/H_2S

Address correspondence to *Csaba Szabo, Department of Anesthesiology, Room 4.2.2H, Bldg # 21, 610 Harborside Drive, Galveston, TX 77555-1102. Phone: 409-772-2222; Fax: 409-772-2222; E-mail: szabocsaba@aol.com.*
Submitted November 23, 2014; Accepted for publication February 18, 2015; Published Online (www.molmed.org) February 18, 2015.

system develops in hyperglycemia/diabetes and tested whether this dysfunction can be corrected by DL-α-lipoic acid (LA), a known antioxidant and 3-MST cofactor (43–45).

MATERIALS AND METHODS

Cell Culture

The bEnd3 microvascular endothelial cell line was purchased from the American Type Culture Collection (Manassas, VA, USA), cultured at 37°C at 5% CO_2, in a humidified chamber, with 5.5 mmol/L glucose containing DMEM (low glucose) or 40 mmol/L glucose (high glucose) with 10% FBS, 2 mmol/L glutamine, 100 IU/mL penicillin, 100 μg/mL streptomycin, and 1% nonessential amino acids. In some experiments, the high glucose cell culture medium was supplemented with 100 μmol/L dihydrolipoic acid (DHLA).

shRNA-Mediated Silencing of 3-MST

bEnd3 cells were transduced at a multiplicity of infection (MOI) of 3 with a lentiviral vector containing shRNA sequences targeting 3-MST (SHCLNV, clone TRCN0000045359). A nontargeting control shRNA sequence (shNT) was used to control for off-target effects (SHC002V, MISSION shRNA; Sigma-Aldrich, St. Louis, MO, USA). Transduced cells were selected and maintained in DMEM media supplemented with puromycin (2 μg/mL). Silencing of 3-MST was confirmed by Western blot analysis of the cell lysates.

Cell Proliferation Assay

bEnd3 cells were grown in full DMEM medium containing 5.5 mmol/L glucose (low-glucose control) or 40 mmol/L glucose (high glucose) for 14 d. Cells were then seeded in 12-well plates at a density of 6×10^3 cells/cm^2. After overnight incubation, cells were exposed to vehicle, 3-MP or NaHS at various concentrations and allowed to proliferate for 48 h. Cells were then harvested and counted using a Neubauer hemocytometer. For real-time assessment of cell proliferation, the xCELLigence system (Roche Diagnostics Corporation, Indianapolis, IN, USA) was used as described (35). Briefly, wild-type, NT shRNA and 3-MST shRNA bEnd3 cells were cultured until approximately 70% confluence in complete medium. Cells were then detached by trypsin–EDTA and resuspended in fresh culture medium at 30,000 cells/mL; 200 μL of this cell suspension was added to each well to yield 6,000 cells/well on an E-Plate 96 (ACEA Biosciences, Inc., San Diego, CA, USA), a specially designed 96-well microtiter plate containing interdigitated microelectrodes to noninvasively monitor the cell proliferation by measuring the relative change in the electrical impedance of the cell monolayer, a unitless parameter named cell index (CI).

Wound Scratch Assay

bEnd3 cells were seeded at 5×10^4 cells/well into a 12-well plate and allowed to reach confluence. Following starvation for 8 h with DMEM containing 0.1% FBS, a scratch was made in a straight line across the diameter of each well by using a 200-μL sterile pipette tip. Cell monolayers were incubated in the presence or absence of 3-MP and NaHS at various concentrations. Images of the monolayers were taken at the start of the experiment and 48 h thereafter using an inverted phase microscope, and the wound sizes were determined by the NIS-Elements imaging software (Nikon, Tokyo, Japan).

Cell Migration Assay

A modified Boyden chamber cell migration assay was used as described (35) in the presence of various concentrations of 3-MP or NaHS. In some experiments, the cell culture medium was also supplemented with 100 μmol/L DHLA. Migration was microscopically quantified at 200× magnification.

Aortic Ring Angiogenesis Assay

The thin gel rat/mouse aortic ring assay was conducted as described (27). Vessel sprouting was stimulated with various concentrations of 3-MP or NaHS. The angiogenic response was measured in the live cultures by counting the number of neovessels.

Western Blot Analysis

bEnd3 cells were lysed in NP-450 lysis buffer (Invitrogen [Thermo Fisher Scientific Inc., Waltham, MA, USA]), diluted in NuPAGE LDS Sample Buffer (Invitrogen [Thermo Fisher Scientific]), sonicated, and boiled. Lysates were resolved on 4%–12% NuPage Bis-Tris acrylamide gels (Invitrogen [Thermo Fisher Scientific]) and transferred to PVDF membranes. Membranes were blocked with Starting Block T20 (Thermo Scientific [Thermo Fisher Scientific]) and then probed overnight with primary antibodies against 3-MST (Atlas Antibodies, Stockholm, Sweden), CSE (Proteintech Group, Inc., Chicago, USA), CBS (Abnova, Taipei City, Taiwan), phosphorylated (Ser473) or total Akt (Cell Signaling Technology, Beverly, MA, USA) and phosphorylated (Ser239) or total VASP (Cell Signaling Technology). Anti-rabbit horseradish peroxidase (HRP) conjugate secondary antibody (Cell Signaling Technology) was applied for 2 h at room temperature. Enhanced chemiluminescent substrate (Pierce Biotechnology, Rockford, IL, USA) was used to detect the signal on high-sensitivity film (Kodak, Rochester, NY, USA). HRP-conjugated antibody against actin (Santa Cruz Biotechnology, Dallas, TX, USA) was used as a loading control. The intensity of Western blot signals was quantified by densitometry using the ImageJ software (NIH, Bethesda, MD, USA; http://rsb.info.nih.gov/ij/).

Measurement of H_2S Production bEnd3 Cells (Live Cells and Cell Homogenates)

To test the effect of hyperglycemia on 3-MST activity H_2S production in live cells, bEnd3 cells were grown in full DMEM media containing 5.5. mmol/L glucose (low glucose) or 40 mmol/L glucose (high glucose) for 14 d. Next, 30,000 bEnd3 cells were seeded in Lab-Tek II chamber coverglass system and incubated overnight. Cells were loaded with 10 μmol/L of the fluorescent H_2S probe 7-azido-4-methylcoumarin (AzMC) for 30 min as described (40). 3-MP was added at various concentrations and cells

were further incubated for 1 h. Cells were washed three times with phosphate-buffered saline (PBS), and the specific fluorescence of the dye was visualized using Nikon Eclipse 80i inverted microscope and NIS-Elements software. In an additional set of studies, 3-MP-induced H_2S production was measured in endothelial cell homogenates using AzMC (10 μmol/L) at 37°C for 1 h, in a 96-well plate format (150 μg total protein per well in 200 μL volume). Control experiments included measurement of 3-MP-induced H_2S production in cell homogenates that have been heat-inactivated (5 min, 100°C) to inhibit enzymatic activity (since 3-MP enzymatic inhibitors are not available). Additional controls included measurement of H_2S production in PBS, in the absence of cell homogenate. Since at higher concentrations, 3-MP induced an increase in AzMC fluorescence, additional studies were conducted where 3-MP solutions (1 mmol/L) were made in PBS in vacutainer tubes and incubated at 37°C for 20 min. In one group of samples, a needle was inserted through the cup to reach the gas phase and connected to a vacuum pump. In the other group of samples, the tubes remained closed. After 20 min, H_2S levels in the solution were measured.

Animals

Male Sprague Dawley rats (~300 g of weight) and male C57BL/6 mice (8 wks of age) were obtained from Charles River Laboratories (Wilmington, MA, USA) or Jackson Laboratories (Bar Harbor, ME, USA) respectively. Animals were housed in an air-conditioned environment (22 ± 1°C, 50 ± 5% relative humidity, 12-h light–dark cycle) with free access to standard chow diet. Animals were allowed five days to acclimatize before the experiments.

In Vivo Angiogenesis Assay

All procedures were approved by the Institutional Animal Care and Use Committee of the University of Texas Medical Branch in accordance with the U.S. National Institutes of Health–approved *Guide for the Care and Use of Laboratory Animals* (46). We performed a 30% total body surface area burn injury in Sprague Dawley rats, as described previously (27). In a first set of experiments, normoglycemic (nondiabetic control) rats were randomly divided into two groups and a full-thickness scald burn was created on their backs under deep anesthesia. Starting at d 1 and for the following 28 d, rats received daily subcutaneous (s.c.) injections of either saline or 3-MP (300 μg/kg per day) in the volume of 100 μl per injection at four equally spaced sites in the transition zone between burn site and healthy tissue. Images of the lesions at d 28 were obtained on a transparent sheet and the areas were quantified by NIS-Elements imaging software. In a subsequent set of experiments, diabetes was induced by streptozotocin (STZ) administered in ice-cold citrate buffer (pH = 4.5) and injected intraperitoneally (IP) at a dose of 60 mg/kg to animals fasted overnight (10). Four days later, development of diabetes was assessed by measuring blood glucose using a glucometer. Seven days after STZ injection, burn wounds were created and wound areas at d 28 of injury was evaluated, as described above for normoglycemic rats. A group of rats received daily LA (100 mg/kg, IP) starting d 1 of burn injury. LA was dissolved as described by Cameron and colleagues (44). The powder was mixed with sterile saline, and NaOH was added until the suspension dissolved. The pH was then brought to pH 7.4 with HCl. Daily s.c. injections of either saline, 3-MP (300 μg/kg/day) or NaHS (300 μg/kg/day) were performed. For the Matrigel plug assay (Corning Matrigel Plug; Corning, Tewskbury, MA, USA), C57BL/6J mice were injected s.c. with 500 μL of Matrigel. 3-MP (300–1000 μg/kg/day) was injected s.c. in proximity of the Matrigel plugs twice a day for 10 d. The Matrigel plugs were recovered by dissection, digested by Drabkin reagent, and angiogenesis was assessed by hemoglobin measurements, as described (27).

Mesenteric Bed Relaxation

The mesenteric bed preparation was performed according to Warner (47). Rats were anesthetized with ketamine/xylazine cocktail. The superior mesenteric artery was cannulated and whole vascular bed perfused for 5 min at 2 mL/min with heparinized (10 IU/mL) and oxygenated (95% O_2, 5% CO_2) Krebs buffer composed of 115.3 mmol/L NaCl, 4.9 mmol/L KCl, 1.46 mmol/L $CaCl_2$, 1.2 mmol/L $MgSO_4$, 1.2 mmol/L KH_2PO_4, 25.0 mmol/L $NaHCO_3$, and 11.1 mmol/L glucose. The mesenteric bed was then isolated, connected to a disposable pressure transducer and changes in perfusion pressure were measured by PowerLab data acquisition software (ADInstruments Inc., Colorado Springs, CO, USA). After approximately 20 min of equilibration, the adrenergic agonist methoxamine was added to the Krebs solution, and relaxation responses to bolus injections of 3-MP (1–100 ng, in 100 μL) were evaluated.

Measurement of Microvascular Blood Flow

Skin microvascular blood flow was measured using a PeriFlux 5000 laser-Doppler flow meter (Perimed Inc., Ardmore, PA, USA). Rats were anesthetized by ketamine/xylazine (IP). The laser-Doppler probe was placed on the shaved dorsal skin of the animals and stable basal signal was recorded. Changes in the s.c. microcirculatory perfusion were detected following intracutaneous injections of either vehicle (saline), 3-MP (0.3–3 mg/kg) or NaHS (0.1–1 mg/kg).

Arterial Blood Pressure Measurement

Rats were anaesthetized by IP injection of ketamine/xylazine cocktail. The left carotid artery was cannulated and connected to a pressure transducer (ADInstruments Inc.). The femoral vein was also cannulated. A heating pad was used to keep the rat's body temperature stable at 37°C. After 60 min of equilibration, bolus injections of increasing doses of 3-MP (0.3-3 mg/kg) or NaHS (0.1–1 mg/kg) were made into the femoral vein with 15 min intervals between injections. Data acquisition and

analysis were accomplished by the PowerLab system.

Plasma H_2S Measurement

3-MP or NaHS were given IP at a dose of 1 mg/kg. Whole blood was collected 30 min later in K_2EDTA blood collection tubes and centrifuged at 4°C for 15 min at 2000*g*. Plasma was isolated and H_2S levels were measured with the fluorescent H_2S probe 7-azido-4-methylcoumarin (AzMC) (40). After incubation of 200 μL of plasma with 10 μmol/L AzMC, the fluorescence was measured using SpectraMax M2 microplate reader (Molecular Devices, Sunnyvale, CA, USA.) at ex = 365, em = 450 nm. H_2S levels were calculated against a NaHS standard curve.

Mitochondrial Isolation and Bioenergetic Analysis

The XF24 Extracellular Flux Analyzer (Seahorse Biosciences, North Billerica, MA, USA) was used to measure mitochondrial bioenergetic function, as described (38). Mitochondria from rat livers (control, diabetic, either treated with vehicle or with LA, as described above) were isolated by differential centrifugation and used for bioenergetic analysis. In the "coupling assay," respiration by the mitochondria (15 μg/well) was sequentially measured in a coupled mitochondrial state with the addition of succinate, as a complex II substrate into the assay media. The detection of basal respiration, state 2 was followed by state 3 (phosphorylating respiration, in the presence of ADP and substrate), state 4 (nonphosphorylating or resting respiration) following conversion of ADP to ATP, finally state 4o was induced with the addition of oligomycin. Next, maximal uncoupler-stimulated respiration (state 3u) was detected by the administration of the uncoupling agent, FCCP. At the end of the experiment the complex III inhibitor, antimycin A was applied to completely shut down the mitochondrial respiration. The coupling assay examines the degree of coupling between the electron transport chain (ETC), and the oxidative phosphorylation (OXPHOS), and can distinguish between ETC and OXPHOS with respect to mitochondrial function/dysfunction. In a separate set of studies, "electron flow" experiments were also conducted. This analysis, which is conducted in mitochondria uncoupled with FCCP (4 μmol/L), allows the functional assessment of selected mitochondrial complexes together in the same time frame. Mitochondrial electron transport was stimulated by the addition of pyruvate and malate (10 mmol/L and 2 mmol/L, respectively, to enable the activity of all complexes), with succinate (10 mmol/L, in the presence of the complex I inhibitor rotenone, 2 μmol/L, to direct the electron flow exclusively through complexes II, III and IV) or with the artificial substrates ascorbate and TMPD (10 mmol/L and 100 μmol/L, respectively, in the presence of the complex III inhibitor antimycin at 4 μmol/L, to selectively activate complex IV). In one set of experiments, the bioenergetic responses from the four groups (control, diabetic, either treated with vehicle or with LA) were analyzed for basal bioenergetic parameters. In another set of experiments (coupling assay), mitochondria were treated with the 3-MST substrate 3-MP (10 μmol/L) *in vitro*, followed by bioenergetic analysis. In an additional set of experiments (coupling assay), mitochondria were treated with DHLA (100 nmol/L) prior to the addition of 3-MP (10 μmol/L), followed by bioenergetic analysis.

Statistical Analysis

Data are shown as mean ± SEM. One-way and two-way ANOVA with Bonferroni multiple comparison test were used to detect differences between groups. Statistical calculations were performed using GraphPad Prism 5 analysis software (GraphPad Software Inc., La Jolla, CA, USA).

RESULTS

3-MP is a Microvascular Relaxant

Bolus administrations of 3-MP (1 to 100 ng in 100 μL volume) to the isolated and perfused mesenteric vascular bed (with functional endothelium and on a stable methoxamine precontractile tone), elicited a concentration-dependent decrease in perfusion pressure (Figure 1A). The vasorelaxant effect of 3-MP on the mesenteric tone was mimicked by NaHS (100 ng bolus in 100 μL volume) (see Figure 1A). With the use of a PeriFlux 5000 laser-Doppler flow meter, we also tested the effect of 3-MP on the skin microvascular blood flow in anesthetized rats. Changes in the s.c. microcirculatory perfusion were detected following intracutaneous injections of either vehicle (saline), 3-MP (0.3-3 mg/kg) or NaHS (0.1–1 mg/kg). Both 3-MP and NaHS relaxed skin microvessels and increased the regional blood flow (Figure 1B). Intravenous bolus injection of 3-MP at 0.3, 1 and 3 mg/kg elicited a transient decrease in the mean arterial blood pressure of anesthetized rats by 6 ± 3, 13 ± 1 and 21 ± 2 mmHg, respectively (Figure 1C). A similar concentration-dependent effect was achieved by intravenous bolus administration of NaHS (0.1–1 mg/kg) (see Figure 1C).

In Vivo Administration of 3-MP Increases Circulating H_2S Levels

IP injection of 3-MP to rats at a dose of 1 mg/kg caused an approximately threefold increase in circulating H_2S levels at 30 min following treatment, as detected in the plasma using a fluorescent probe. NaHS (1 mg/kg), which was used as a positive control, increased circulating H_2S levels as well (Figure 1D).

The Proangiogenic Effect of 3-MP *In Vitro* Is Associated with the Activation of Akt and Protein Kinase G (PKG)

3-MP elicited a concentration-dependent increase in microvessel sprouting in rat aortic rings (Figure 2A). In bEnd3 microvascular endothelial cells, 3-MP facilitated migration, as measured by the wound scratch or the transwell migration assays (Figures 2B, C) and stimulated endothelial cell proliferation (Figure 2D). Similarly, and in line with prior findings (27), NaHS (30 μmol/L) induced proangiogenic responses *in vitro*. 3-MP

(at 100 μmol/L, the concentration that caused maximal proangiogenic responses *in vitro*) stimulated Akt phosphorylation at its activating site (Ser473) in bEnd3 cells (Figure 2E). Silencing of 3-MST by shRNA lentiviral particles (inset in Figure 2F) resulted in a significant inhibition of the proliferation rate of bEnd3 cells, as measured by the xCELLigence system (see Figure 2F), pointing to the importance of the endogenous 3-MP/3-MST/H_2S pathway in the maintenance of endothelial cell angiogenesis. Cells with 3-MST silencing showed lower levels of activated Akt (phosphorylated at Ser473) and phospho-VASP (Ser239), a marker of PKG activation, compared with the controls (wild-type cells or cells treated with a scrambled, nontargeting shRNA sequence) (Figures 2G, H).

Contribution of Enzymatic and Nonenzymatic H_2S Production to the Effects of 3-MP

In an additional set of studies, 3-MP-induced H_2S production was measured in bEnd3 endothelial cell homogenates. 3-MP induced a concentration-dependent increase in AzMC fluorescence (Figure 3A). When the homogenates have been heat-inactivated (5 min, 100°C) to inhibit enzymatic activity, the H_2S signal was reduced, but not completely blocked (especially at the two highest concentrations tested, 1 and 3 mmol/L) (see Figure 3A). Likewise, higher concentrations of 3-MP induced some increase in AzMC fluorescence in PBS, in the absence of cell homogenate (see Figure 3A). Therefore, additional studies were conducted in which 3-MP solutions were made in PBS and either closed down with no headspace, or left open and connected to a vacuum system for 24 h to remove gaseous products diffusing into the headspace, followed by the measurement of H_2S levels in the solution. These studies showed that the H_2S signal was reduced when the solution's headspace gases were removed via a vacuum system (Figure 3B), lending further proof that 3-MP at high concentrations gives rise to H_2S via a nonenzymatic mechanism. However, the fact that this production requires high concentrations of 3-MP makes it unlikely that this process has a major contribution to the cellular responses we have observed in the current study.

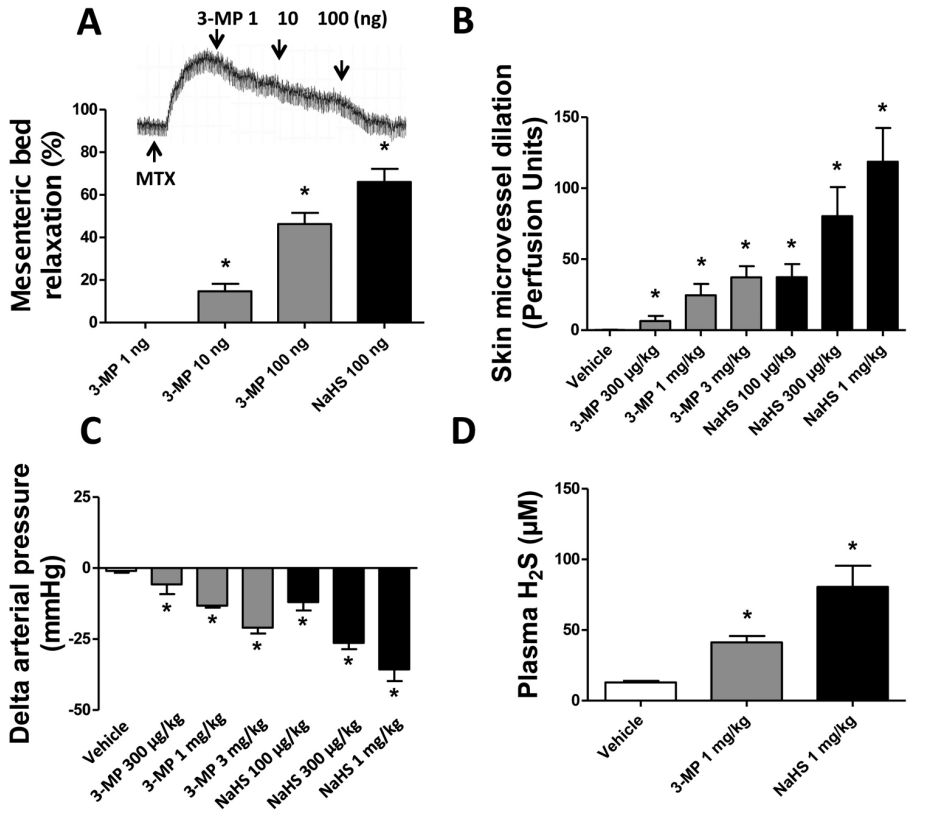

Figure 1. 3-MP mimics the vasorelaxant properties of H_2S. (A) Similarly to NaHS, 3-MP elicits decreases in perfusion pressure (vasorelaxation) in preconstricted mesenteric arterial bed in a concentration-dependent manner. Test agents were administered as successive boluses (each in 100 μL volume). The inset shows a typical vasorelaxation curve to 3-MP as recorded by PowerLab data acquisition software (*$p < 0.05$, n = 4/group). (B) 3-MP, similarly to NaHS, induced skin microvessel dilation as measured by a PeriFlux 5000 laser-Doppler flow meter placed on the shaved dorsal skin of anesthetized animals (*$p < 0.05$ versus vehicle, n = 4/group). (C) 3-MP, similar to NaHS, induces concentration-dependent decreases in blood pressure in anaesthetized rats. The left carotid artery was cannulated and connected to a pressure transducer (ADInstruments) to detect changes in the arterial blood pressure. Intravenous bolus injection of 3-MP at 0.3, 1 and 3 mg/kg of body weight and NaHS at 0.1, 0.3 and 1 mg/kg of body weight elicited transient decreases in mean arterial blood pressure (*$p < 0.05$ versus vehicle; n = 3/group). (D) IP injections of 3-MP at 1 mg/kg to rats resulted in increased circulating levels of H_2S as measured by the AzMC fluorescent probe at 30 min; the circulating H_2S response to the injection of NaHS is shown as a positive control (*$p < 0.05$ versus vehicle; n = 3/group). In all bar graphs, mean ± SEM values are shown.

3-MP Exerts Proangiogenic Effects *In Vivo*

Daily topical injections of 3-MP (0.3 and 1 mg/kg) caused a sustained increase in neovascularization (measured by hemoglobin content) in Matrigel plugs implanted for 10 d in C57BL/6 mice (Figures 4A, B). Because wound healing is dependent on angiogenesis, we next assessed the ability of 3-MP to facilitate wound closure in a burn wound model in the rat. Skin wound sizes, measured by planimetry at d 28, were markedly reduced in rats receiving

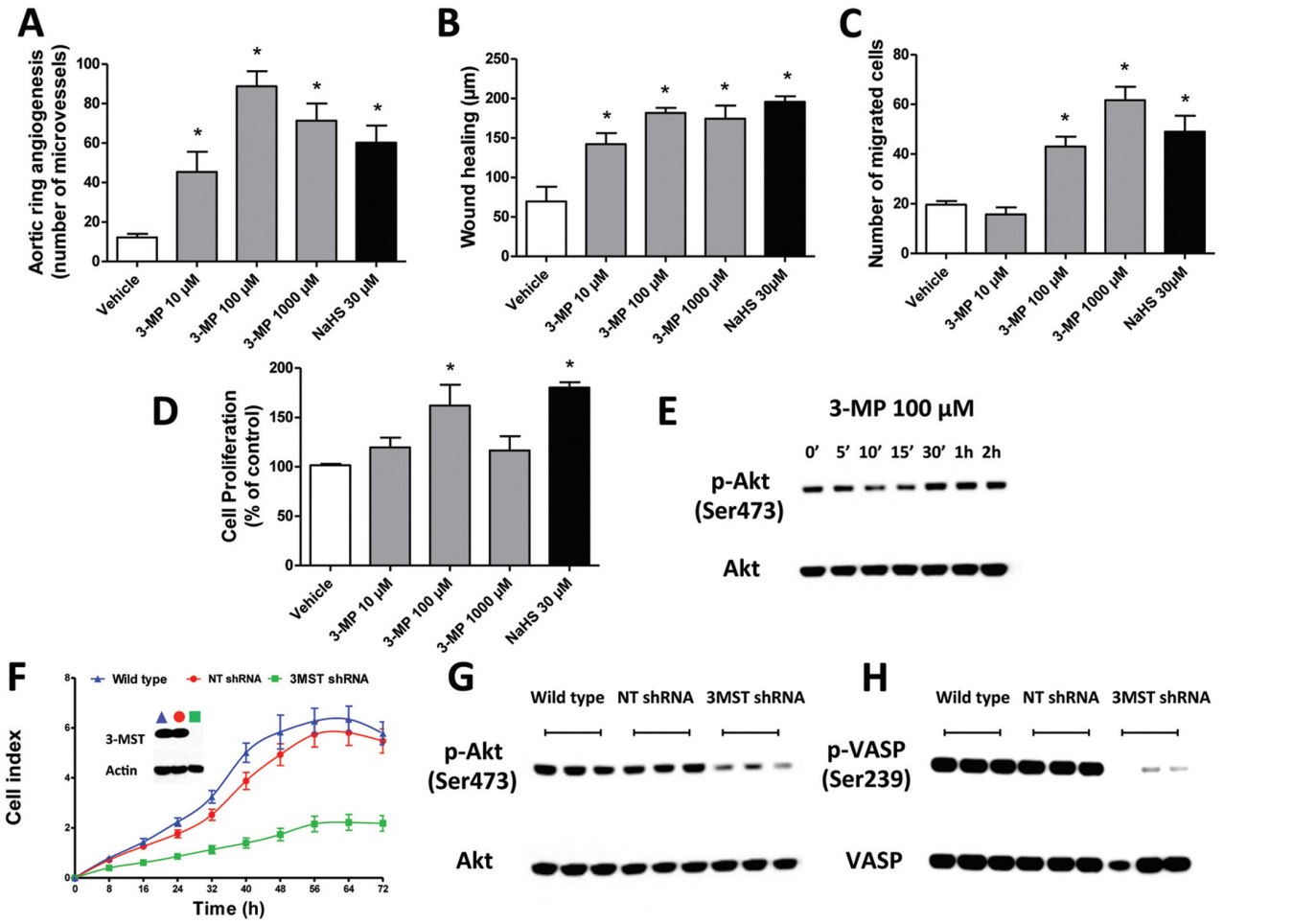

Figure 2. 3-MP mimics the proangiogenic property of H_2S. (A) Aortic rings were harvested from rats and cultured for 7 d in collagen gel in Opti-MEM medium containing 1% FBS in the presence or absence of 3-MP (10 μmol/L to 1 mmol/L) or NaHS (30 μmol/L), followed by the quantification of microvessels. Both 3-MP and NaHS increased microvessel formation (*$p < 0.05$ versus vehicle; n = 4/group), although at the increase of 3-MP from 100 μmol/L to 1 mmol/L did not elicit an additional increase in microvessel formation; in fact, a tendency for a decrease was noted. This type of concentration response is consistent with the often-reported bell-shaped pharmacological effect of H_2S where higher concentrations exert inhibitory effects on various cell functions. (B) bEnd3 cells were seeded in 12-well plates and cultured overnight. Following starvation, a wound scratch was made. Cells were subsequently incubated with 3-M (10 μmol/L to 1 mmol/L) or NaHS (30 μmol/L) for an additional 48 h, followed by the evaluation of scratch wound healing (μm). Both 3-MP and NaHS facilitated scratch wound healing responses (*$p < 0.05$ versus vehicle; n = 4/group). (C–D) The effects of 3-MP (10 μmol/L to 1 mmol/L) or NaHS (30 μmol/L) on bEnd3 cell migration (C) and cell proliferation (D). Both 3-MP and NaHS facilitated these responses (*$p < 0.05$ versus vehicle; n = 4/group), although at the highest concentration of 3-MP, the cell proliferation response was no longer stimulated, consistent with the often-reported bell-shaped pharmacological effect of H_2S, where higher concentrations exert inhibitory effects on various cell functions. (E) bEnd3 cells were exposed to 100 μmol/L 3-MP for the indicated times. Cell lysates were analyzed by SDS/PAGE. PVDF membranes were blotted by using rabbit polyclonal antibodies against phosphorylated (Ser473) or total Akt. Increased levels of phosphorylated Akt were detected upon 3-MP treatment, starting at 30 min. The blot shows a representative experiment of n = 3 independent determinations conducted on different experimental days (F) The lentiviral shRNA vector targeting 3-MST was transfected into bEnd3 cells. The shRNA vector effectively inhibited the expression of 3-MST gene at the protein level, as shown by Western blot analysis (inset in F). Following 3-MST silencing, cells were seeded at the density of 3,000 cells per well in xCELLigence plates and proliferation was monitored for 72 h. Downregulation of 3-MST markedly reduced the proliferation rate of the bEnd3 cells. The graph shows a representative experiment of n = 3 independent determinations conducted on different experimental days; each data point represents mean ± SEM of n = 6 xCELLigence wells. (G–H) Cell lysates from wild-type cells, nontargeting (NT) shRNA cells and 3-MST shRNA cells were analyzed by SDS/PAGE and the analysis of the blots revealed low detectable levels of (G) phosphorylated Akt (ser473) and (H) phosphorylated VASP (ser239), a marker of protein kinase G activation. There was an inhibition of both of these responses in cells with 3-MST downregulation. The blots show a representative experiment of n = 3 independent determinations conducted on different experimental days. In all bar graphs, mean ± SEM values are shown.

daily topical administrations of 3-MP at 0.3 mg/kg (Figures 4C, D).

Hyperglycemia Impairs the 3-MP/3-MST/H_2S Pathway

To test the effect of hyperglycemia on the expression and activity of 3-MST, bEnd3 cells were grown in full DMEM medium containing 5.5 mmol/L glucose (low glucose) or 40 mmol/L glucose (high glucose) for 14 d. Cell lysates were then analyzed by Western blotting. No differences were found in the expression levels of 3-MST in bEnd3 cells following 14 d of hyperglycemia. Similarly, and in line with our previous findings (10), no effect of hyperglycemia was found on the expression of cystathionine-γ-lyase (CSE), another enzymatic source of H_2S in endothelial cells. A tendency for a hyperglycemia-induced increase in the levels of cystathionine-β-synthase (CBS, a third H_2S-producing enzyme) was noted (Figure 5A). Using the fluorescent H_2S probe AzMC, we tested the effect of hyperglycemia (14 d of incubation at 40 mmol/L glucose) on 3-MST activity (defined as the ability to convert the substrate 3-MP to H_2S) in live bEnd3 cells. Cells grown in low glucose conditions and treated with 3-MP (10 or 100 μmol/L) showed an increase in the intracellular fluorescence signal, indicating increased 3-MST-dependent enzymatic production of H_2S. Hyperglycemic cells showed a marked decrease in the detection of intracellular fluorescent signal (Figure 5B), which can be interpreted as a reduced ability of 3-MST to convert 3-MP to H_2S when the extracellular glucose concentration is elevated. We observed an impairment of the proangiogenic properties of 3-MP in hyperglycemic bEnd3 cells, as well. After 14 d of hyperglycemia, 3-MP was no longer able to stimulate angiogenesis, as assessed by cell proliferation, wound scratch healing and cell migration in bEnd3 cells (Figures 5C–E). Moreover, 3-MP failed to facilitate wound closure in the burn wound model in STZ-diabetic rats (Figure 5F). By contrast, the H_2S donor NaHS maintained its proangiogenic and wound-healing-stimulating activity in hyperglycemic cells and in diabetic animals (see Figures 5C–F).

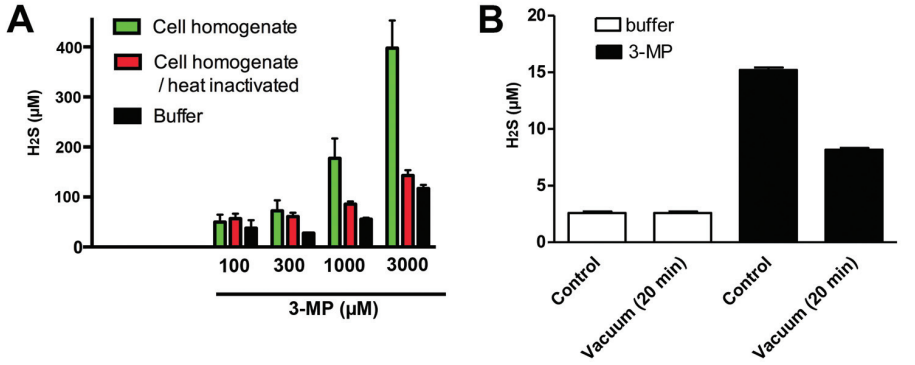

Figure 3. Enzymatic and nonenzymatic H_2S production from 3-MP. (A) bEnd3 cell homogenates, heat-inactivated homogenates or PBS in the absence of homogenates were incubated with increasing concentrations of 3-MP for 1 h, followed by the measurement of H_2S production. (B) Effect of removal of headspace gases to the detectable levels of H_2S in a PBS solution of 3-MP (1 mmol/L). Data show mean ± SEM values; n = 3 independent determinations.

Lipoic Acid Restores the Proangiogenic Effect of 3-MP in Hyperglycemia and Diabetes

LA, a naturally occurring dithiol compound, is known as an antioxidant and an essential cofactor of mitochondrial enzymes (44,45). LA directly terminates free radicals and chelates transition metal ions. Recent studies showed that LA acts as a stimulator/cofactor of 3-MST (43). To test whether LA may improve or restore the proangiogenic effect of 3-MP in hyperglycemia, bEnd3 cells were grown in hyperglycemia (40 mmol/L glucose) for 14 d in presence or absence of 100 μmol/L of the reduced form of LA (DHLA). DHLA restored the effect of 3-MP to stimulate bEnd3 endothelial cell migration in hyperglycemia (see Figure 5E). To test the effect of lipoic acid *in vivo*, STZ-diabetic rats were subjected to the burn wound healing model. Rats also received either vehicle or LA administrations (100 mg/kg, IP daily), starting 7 d following STZ injection and continuing for an additional 28-d period. 3-MP or NaHS was given locally in a fashion identical to the studies discussed in Figure 3. The ability of 3-MP to enhance the wound closure was restored by LA treatment in STZ-diabetic rats (see Figure 5F).

Diabetes Elicits Marked Alterations in Mitochondrial Function

Consistent with prior reports (48–51), mitochondria isolated from STZ-diabetic animals showed marked functional alterations (in most cases, suppression) in mitochondrial function. The nature of the alterations depended on the mitochondrial parameter studied and the assay employed. Figures 6A and C represent original tracings of a coupling and electron flow bioenergetic assays, respectively, as conducted in liver mitochondria obtained from healthy control versus STZ-diabetic rats. Figures 6B and D show collected data of five individual measurements conducted on different experimental days. Data presented in panels A and B show the comparison of mitochondrial function between normal and diabetic mitochondria in the coupling experiment, during which the assay media contains succinate (a mitochondrial complex II substrate) and rotenone (a mitochondrial complex I inhibitor). In this assay, electron flow initiates from complex II and runs over complexes III and IV. Serial measurements of basal/state 2, state 3, state 4o and the uncoupler-stimulated respiration, state 3u, were performed

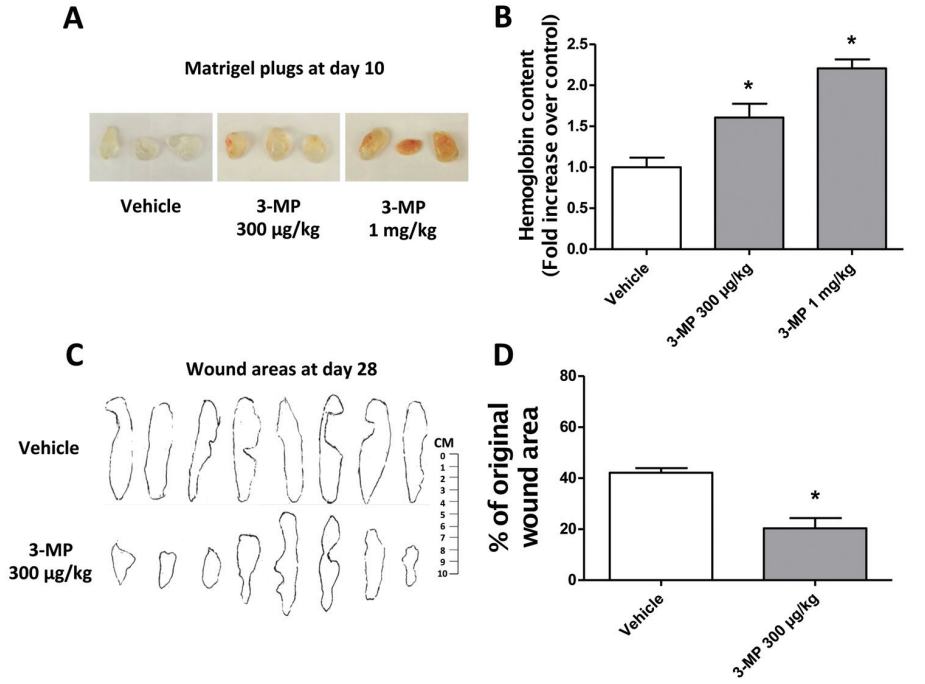

Figure 4. Stimulatory effects of 3-MP on angiogenesis *in vivo*. (A–B) The effect of 3-MP on angiogenesis *in vivo* was assessed by Matrigel plug assay in C57BL/6 mice. Daily 3-MP treatments (0.3 and 1 mg/kg) significantly promoted neovascularization in the Matrigel plug assay. (A) Images of the Matrigel plugs immediately after collection at d 10 are shown. (B) Neovascularization in the Matrigel plugs was quantified by measuring hemoglobin content using Drabkin reagent, demonstrating the stimulatory effect of 3-MP on angiogenesis (*$p < 0.05$ versus vehicle; n = 5/group). (C–D) Following anesthesia and analgesia, rats were placed in a mold and subjected to burn injury by submerging the back in scalding (96–99°C) water for 10 s. Rats were randomly divided into two groups and treated daily for 28 d either with vehicle or 3-MP (300 µg/kg per day s.c.). Subcutaneous injections of 3-MP were performed daily at four equally spaced sites in the transition zone between burn site and healthy tissue. (C) Burn wound areas were determined on d 28 by NIS-Elements imaging software (Nikon) and (D) were quantified and analyzed statistically. 3-MP administration significantly reduced the wound area (*$p < 0.05$ versus vehicle; n = 8/group). In all bar graphs, mean ± SEM values are shown.

through the sequential injections of ADP, oligomycin, FCCP and antimycin A. All respiration stages significantly differed between control and STZ-diabetic mitochondria, with the oxygen consumption rate (OCR) values in basal (state 2), state 3 and state 4o being higher in STZ group than in the control group, while state 3u (which arises after the addition of the uncoupling agent FCCP) STZ-diabetic mitochondria showed a reduction in their peak mitochondrial function. In panels C and D, the results of an "electron flow assay" are shown, which evaluates the electron flow activity through all four complexes of the mitochondrial electron transport chain. The assay media contains pyruvate and malate as substrates of complex I, and the bioenergetic measurement is conducted in the presence of FCCP to uncouple the mitochondria. In this assay, each mitochondrial complex can be examined individually, the sequential injection of rotenone, succinate, antimycin and TMPD/ascorbate permits the evaluation of the functions of complexes I, II and IV. When the function of all complexes (CI + CII + CIII + CIV) was intact, or when complex I was selectively inhibited or when the functionality of complex IV was assessed on its own, isolated mitochondria collected from STZ diabetic rats exhibited a marked suppression of function (Figure 6).

The Mitochondrial Activity of the 3-MST/H_2S Pathway Is Reduced in Diabetes with Restoration by Lipoic Acid

Because in the coupling assay the most marked and most consistent differences between control and diabetic animals were noted in the FCCP-induced increases in oxygen consumption (which yields the bioenergetic parameter usually described as "respiratory reserve capacity") (see Figure 6), in the followup studies we have concentrated on this parameter. 3-MP (10 µmol/L) stimulated mitochondrial function, consistent with our recent studies (20,38), showing that mitochondria generate H_2S when incubated with 3-MP and that the resulting H_2S gives electrons to the mitochondria at complex II and stimulates mitochondrial electron transport and cellular bioenergetics. The 3-MP-elicited stimulatory effect on mitochondrial respiration was reduced in mitochondria from STZ-diabetic rats by approximately 40% (Figure 7), in line with prior findings (20) demonstrating that oxidative stress attenuates the catalytic activity of 3-MST and of the H_2S-associated bioenergetic responses. Treatment of the nondiabetic animals with LA did not affect their mitochondrial function (Figure 7A), but it improved the function of the STZ-diabetic mitochondria (Figure 7B). In addition, treatment with LA *in vivo* or with DHLA *in vitro* (or, most, effectively, combined treatment with *in vivo* LA and *in vitro* DHLA) enhanced/partially restored the bioenergetic stimulatory effect of 3-MP in the mitochondria isolated from diabetic animals (Figure 8). The seven open bars in the left side of the figure represent the responses of mitochondria isolated from livers of nondiabetic animals; the seven closed bars in the right side of the figure represent the bioenergetic responses of mitochondria isolated from livers of STZ-diabetic animals. The FCCP-induced increments in vehicle-treated

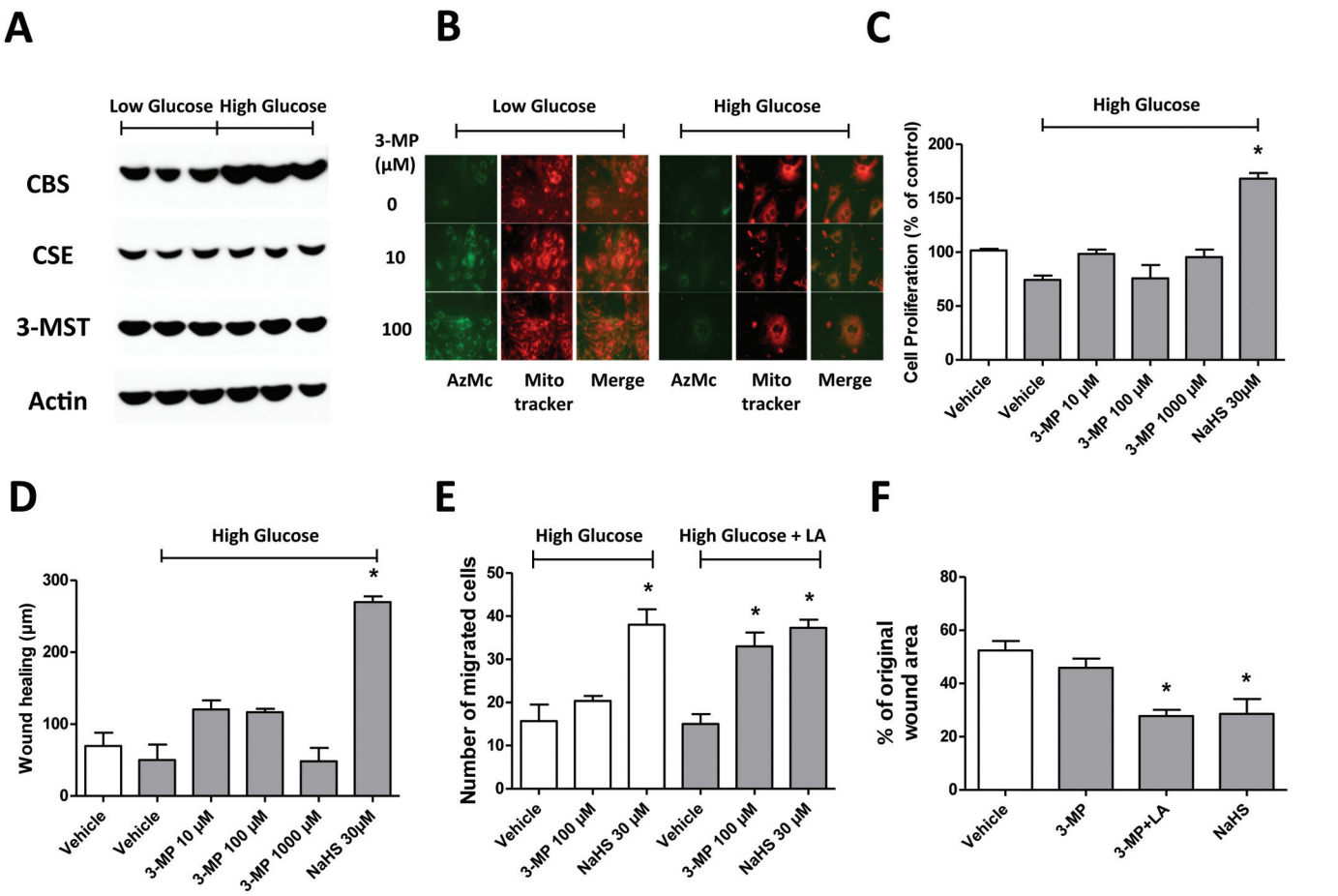

Figure 5. Hyperglycemia reduces 3-MST activity without affecting 3-MST protein expression. (A) bEnd3 cells were grown in full DMEM media containing 5.5. mmol/L glucose (low-glucose) or 40 mmol/L glucose (high glucose) for 14 d. Cell lysates were then analyzed by Western blotting. No differences were found in the expression levels of 3-MST and CSE in bEnd3 cells following 14 d of hyperglycemia, while a tendency for increased levels of CBS was noted. The blots show a representative experiment of n = 3 independent determinations conducted on different experimental days. (B) The H_2S probe AzMC was employed to measure 3-MST activity (estimated as the ability to convert the substrate 3-MP (10–100 μmol/L) to H_2S) in live bEnd3 cells. Cells grown in high glucose conditions, unlike those grown in normal glucose, showed a marked decrease in the intracellular fluorescent signal stimulated by 3-MP. The figures show a representative experiment of n = 3 independent determinations conducted on different experimental days. Colocalization studies with the mitochondrial localization marker Mitotracker show that 3-MP-induced H_2S production shows partial mitochondrial localization, consistent with the known presence of 3-MST both in the mitochondria and in the cytoplasm. (C–E) Functional impairment of the 3-MP/3-MST/H_2S pathway was further evidenced by the loss of the *in vitro* proliferative, wound-healing-stimulatory and scratch-wound-closing-stimulatory effect of 3-MP in hyperglycemic bEnd3 cells (experimental conditions as in Figure 2). Note that 3-MP no longer stimulates these responses, while NaHS continues to exert a significant effect (*$p < 0.05$ versus vehicle; n = 4/group). (E) The presence of LA restored the stimulatory effect of 3-MST on bEnd3 cell migration in high glucose conditions (*$p < 0.05$ versus vehicle; n = 4/group), but did not affect the effect of NaHS. (F) In STZ-diabetic rats subjected to burn-induced wound healing model, 3-MP did not accelerate wound closure, whereas the combination of LA and 3-MP had a significant effect. Similar to its effect in nondiabetic rats, NaHS remained effective in stimulating burn wound healing in diabetic animals. Burn wound healing in STZ-diabetic animals was studied and analyzed similar to the approach used in nondiabetic rats in Figure 4. (*$p <$ 0.05 versus vehicle; n = 8/group). In all bar graphs, mean ± SEM values are shown.

control mitochondria (for the groups indicated with open bars) or in vehicle-treated STZ-diabetic mitochondria (for the groups indicated with closed bars) were considered as FCCP-induced respiration in normal conditions and were subtracted from all the 3-MP/DHLA/LA-mediated bioenergetic responses shown in the figure. For instance, the white bar on the left (DHLA, with a value very close to zero) means that the respiratory reserve capacity of the mitochondria was unaffected by the *in vitro* addition of DHLA in control (nondiabetic) mitochondria. Likewise, the black bar on the right with a high value (LA +

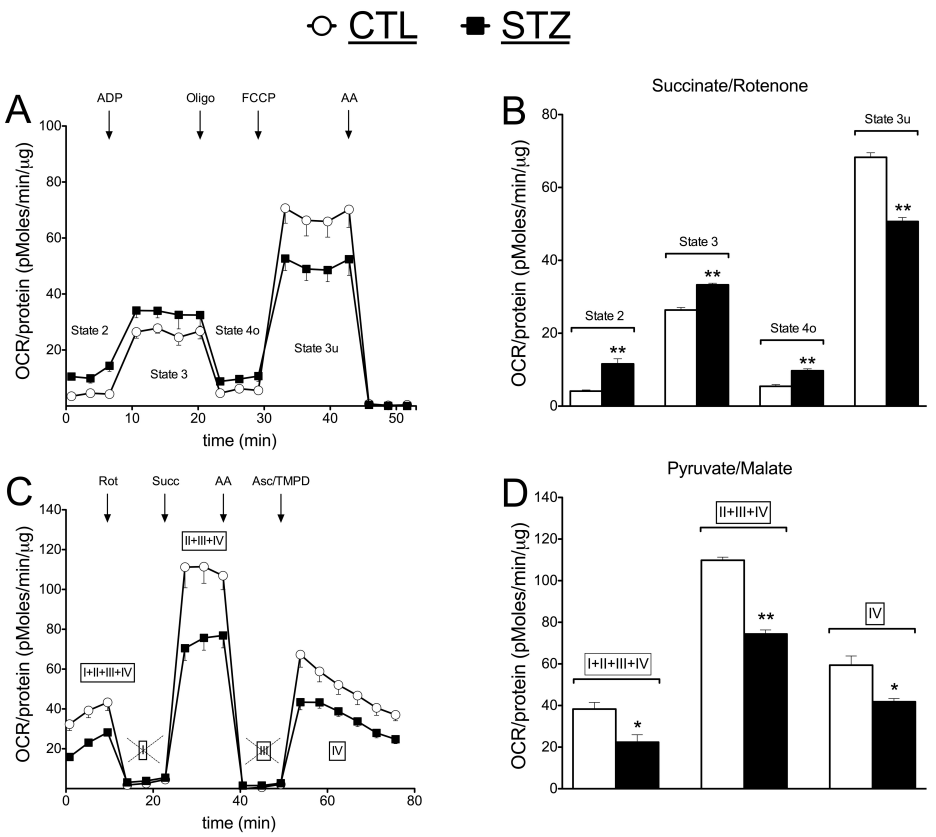

Figure 6. Altered mitochondrial function in liver mitochondria of STZ-diabetic rats. Comparison of mitochondrial oxygen consumption rate (OCR) of liver mitochondria isolated from control (CTL) and streptozotocin-diabetic (STZ) rats is shown in (A,B) coupling and (C,D) electron flow experiments. Note the suppression of the FCCP-induced oxygen consumption responses (respiratory reserve capacity, state 3u) by diabetes in the coupling experiment, and the suppression of all bioenergetic parameters in the electron flow experiment. A–B show measurement of bioenergetics tracings and C–D show mean ± SEM values collected from five individual measurements conducted on different experimental days; $^{**}p < 0.01$ shows significant differences between control and diabetic mitochondria for the indicated functional parameter.

DHLA + 3-MP) means that the indicated condition (*in vivo* lipoic acid treatment of STZ-diabetic rats, followed by *in vitro* DHLA and 3-MP administrations) markedly elevated the respiratory reserve capacity, when compared with the control STZ-diabetic mitochondria (see Figure 8).

DISCUSSION

The main novel results of the present report are the following: (a) the 3-MP/3-MST/H_2S pathway regulates vascular function (acts as a microvascular vasorelaxant); (b) the 3-MP/3-MST/H_2S pathway acts as a physiological stimulator of angiogenesis; (c) the 3-MP/3-MST/H_2S pathway develops a functional impairment in hyperglycemia (suppression of the angiogenic and bioenergetic responses); and (d) lipoic acid improves/restores the function of the 3-MP/3-MST/H_2S pathway in hyperglycemia. On the basis of these findings, we speculate that the impairment of the 3-MP/3-MST/H_2S pathway may contribute to the pathogenesis of hyperglycemic endothelial cell dysfunction. We also speculate that pharmacological supplementation of H_2S and/or the restoration of the 3-MST system may be a potential future experimental therapeutic approach. It is conceivable that some of the previously noted beneficial and therapeutic effects of lipoic acid in diabetic complications (including vascular disease and diabetic neuropathy) (44,45,52,53) may be, at least in part, related to the lipoic acid–induced enhancement of the H_2S pathway in diabetic animals or diabetic patients.

The 3-MP/3-MST pathway is receiving increasing attention as a novel enzymatic system involved in physiological H_2S generation (with CSE and CBS being the other two physiological H_2S-generating enzymes, which have been studied for longer times and are currently much better characterized). Although the presence of 3-MST and the metabolism of 3-MP by 3-MST in various tissues has been known for over three decades (54), the production of H_2S by this pathway has only been realized in the last few years. There are now several reports demonstrating 3-MP/3-MST induced H_2S production in the central and peripheral nervous system (55,56) and in the vascular endothelium (17), as well as in various other cells and tissues (20,38,43). The oxidative-stress-sensitive nature of 3-MST (57,58) and the functional consequence of this property (in terms of reduced H_2S production and impaired cellular bioenergetics) (20) have also been demonstrated in recent years. Moreover, the molecular structure and biochemical profile of the human 3-MST enzyme has recently been characterized in significant detail (59). However, the physiological and especially the pathophysiological relevance of the 3-MP/3-MST/H_2S pathway remains largely unexplored. A study by Shibuya and colleagues that demonstrated H_2S production by 3-MP via 3-MST in endothelial cells focused on the localization of the enzyme within the endothelium and the biochemical aspects of H_2S production, but did not explore the functional consequences of the H_2S produced by 3-MST. The results of the present study, demonstrating that 3-MP induces microvascular relaxation, angiogenesis and *in vivo* H_2S production extend the prior findings and suggest that 3-MST-derived H_2S, in addition to CBS- and CSE-derived H_2S plays physiological regulatory roles in the cardiovascular sys-

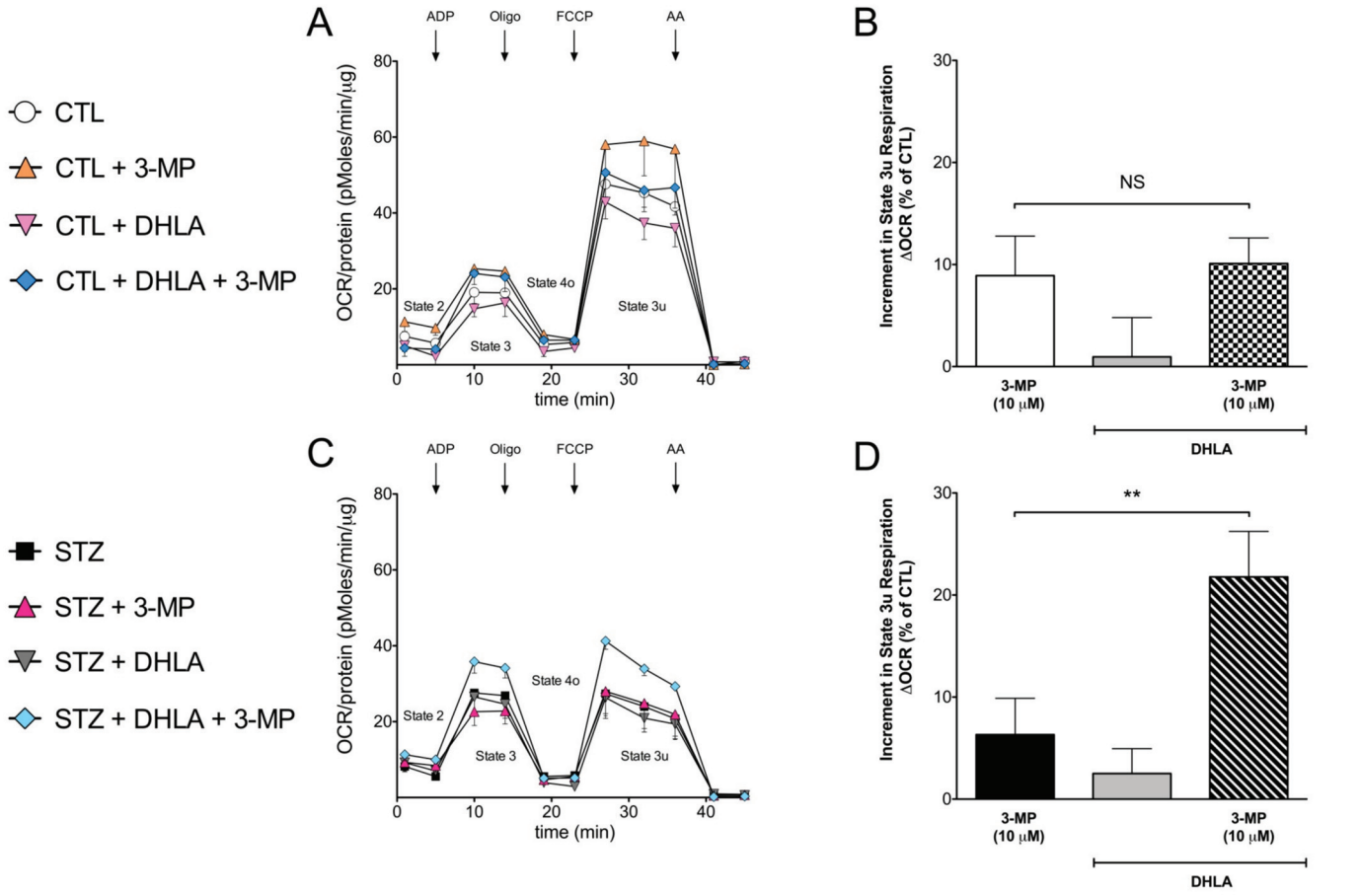

Figure 7. 3-MP/3-MST mediated bioenergetic responses are suppressed in liver mitochondria of STZ-diabetic rats; restoration of the responses by DHLA *in vitro*. (A–D) Comparison of mitochondrial oxygen consumption rate (OCR) of liver mitochondria isolated from control (CTL) and streptozotocin-diabetic (STZ) rats, with or without the addition of 3-MP (10 μmol/L), in the presence or absence of preincubation with DHLA is shown in mitochondrial coupling assay experiments. (A,C) representative bioenergetic tracings; (B,D) collective OCR values (from six individual measurements conducted on different experimental days) show increments in the 3-MP-induced increases in bioenergetic responses (calculated as increments in area-under-the-curve (AUC) of the calculated respiratory reserve capacity responses after FCCP administration) in mitochondria isolated from control or STZ-diabetic rats, and in mitochondria of STZ-diabetic rats with or without DHLA (100 nmol/L) incubation. Note the suppression of the 3-MP induced bioenergetic responses in mitochondria from STZ-diabetic rats, and the stimulatory effect of DHLA in mitochondria isolated from STZ-diabetic (but not in mitochondria isolated from control) rats. Bar graphs show mean ± SEM values; $^{**}p < 0.01$ shows significant differences between 3-MP treated and 3-MP combination with DHLA-treated diabetic mitochondria *in vitro* between the two indicated groups; NS: not significant.

tem as a vasodilator and proangiogenic local hormone. The reduced proliferative capacity of the 3-MST-silenced endothelial cells, shown in the current study, indicates a significant role of the 3-MP/3-MST/H_2S system in the physiological maintenance of angiogenesis. This effect may be due to a combination of the stimulation of H_2S-mediated signaling pathways (such as Akt and PKG, as well as, potentially, many other pathways) and H_2S-mediated stimulatory bioenergetic effects (to contribute to the generation of ATP, the biological "fuel" needed for cell proliferation, movement and division). It should be emphasized that, similar to the case with the other two H_2S-producing enzymes CSE and CBS, there may be marked differences in the expression and activity of 3-MST in different vascular beds, blood vessels of different sizes and different species. Therefore, additional studies (including studies in 3-MST deficient mice) are needed to extend the physiological importance and the overall applicability of the current findings.

With respect to the pathophysiological roles of the 3-MP/3-MST/H_2S system, the literature is scarce. We have recently made the observation that physiological aging impairs the bioenergetic effect of 3-MP (21), Wallace and colleagues demonstrated the upregulation of 3-MST in colonic inflammation (60), several groups showed the upregulation of 3-MST in response to various forms of hypoxia

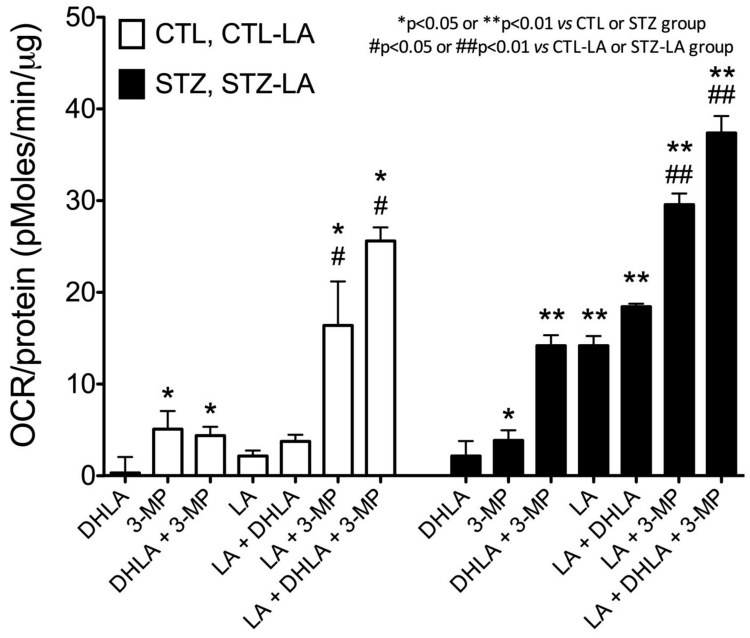

Figure 8. Treatment of STZ-diabetic rats with LA enhances the bioenergetic function of rat liver mitochondria; comparison with *in vitro* treatment of the mitochondria with DHLA. (A–B) Comparison of the respiratory reserve capacity (FCCP-induced increments in oxygen consumption rate (OCR)) of rat liver mitochondria isolated from control animals or from STZ-diabetic animals treated with either vehicle or LA *in vivo*, with or without additional *in vitro* preincubation with DHLA (100 nmol/L) in mitochondrial coupling assay experiments. The height of each bar corresponds to the magnitude of the increase in respiratory reserve capacity by the indicated condition, expressed as delta AUC. Please note that the most pronounced enhancements in 3-MP-induced bioenergetic responses were seen in the presence of LA or LA + DHLA pretreatments. When these treatments were applied, the 3-MP bioenergetic responses of the STZ-diabetic rats became higher than the responses of the corresponding nondiabetic controls, indicating that these treatments tended to restore normal mitochondrial functionality. Please also note that LA treatment of the STZ-diabetic rats (but not the control rats) increased mitochondrial function in the absence of any 3-MP addition. $^{*}p < 0.05$ and $^{**}p < 0.01$ show significant enhancements of FCCP-induced OCR responses by the indicated agents (*in vitro* 3-MP; *in vitro* DHLA in the presence of *in vitro* 3-MP; *in vivo* LA; *in vivo* LA, followed by the addition of *in vitro* DHLA; *in vivo* LA, followed by the addition of *in vitro* 3-MP; *in vivo* LA, followed by the addition of *in vitro* DHLA and 3-MP) compared with FCCP alone in the respective (control or STZ-diabetic) mitochondria; $^{\#}p < 0.05$ and $^{\#\#}p < 0.01$ show significant enhancements of FCCP-induced OCR responses by *in vitro* 3-MP or *in vitro* DHLA and 3-MP in combination, when compared with the responses of the respective (control or STZ-diabetic) mitochondria isolated from LA-treated rats. Bar graphs show mean ± SEM values of at least n = 4 experiments for each condition.

(61,62), and there is a recent report showing the downregulation of 3-MST in stroke (63). Moreover, a recent report showed that 3-MST-knockout mice exhibit increased anxiety-like behaviors (64), although there are currently no published data with respect to the nature of the changes in the H_2S homeostasis in the 3-MST-knockout mice. Likewise, prior to the present report, there were no papers in the literature connecting the 3-MP/3-MST/H_2S system to the hyperglycemia or diabetic complications. The findings presented in the current report indicate that the function (but not the expression level) of 3-MST is decreased in STZ-diabetes *in vivo* and during elevated extracellular glucose in endothelial cells *in vitro*. One of the key features that elevated extracellular glucose *in vitro* and STZ-diabetes *in vivo* share is the increased cellular production of reactive oxygen and nitrogen species as these species have been long identified as key pathophysiological factors in mitochondrial dysfunction, endothelial dysfunction and the development of micro- and macrovascular dysfunction and mitochondrial dysfunction in diabetes (48–51). Because the functionality of the 3-MST system was improved/restored by treatment with lipoic acid both *in vitro* and *in vivo*, we believe that oxidative stress is the most likely mechanism through which diabetes (or hyperglycemia) impairs the catalytic activity of 3-MST (Figure 9). Interestingly, the proangiogenic and wound-healing stimulatory effect of authentic H_2S (generated from NaHS) was not attenuated by hyperglycemia. This indicates that the signaling and effector pathways downstream from H_2S are not impaired significantly in experimental models used in the current study. It must be noted that, depending on the experimental conditions and models used, the other H_2S-producing enzyme systems also have been shown to be affected by diabetes and diabetic complications (8–15,65–67; overviewed in [67]). Thus, it is likely that there is a complex dysregulation of the H_2S system in diabetes, the nature of which depends on the model used, as well as the stage and severity of the disease.

CONCLUSION

The current results further support the view (67) that authentic H_2S donors have future therapeutic potential in conditions associated with hyperglycemia. While the current report utilized an STZ model of diabetes, hyperglycemia is also important in the pathophysiological context of critical illness (for example, acute hyperglycemia post-surgery) (68). Likewise, the wound healing studies reported here were discussed in the context of diabetes, but wound healing is also highly relevant in the context of critical illness (burn injury) (69,70).

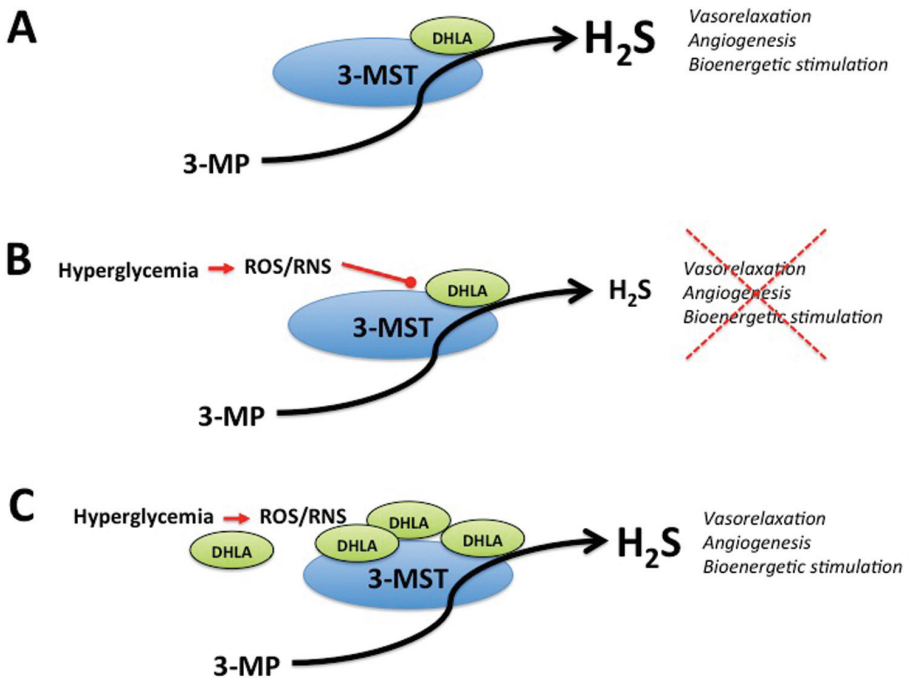

Figure 9. Impairment of the 3-MP/3-MST system in hyperglycemia/diabetes; restoration by lipoic acid (DHLA) proposed mechanisms. (A) Normal conditions, physiological levels of endogenous DHLA permit the normal function of 3-MST, yielding H_2S production from 3-MST. (B) Hyperglycemic conditions, overproduction of reactive oxygen and nitrogen species (ROS, RNS) impairs the 3-MP/3-MST system, by consuming DHLA, and/or by directly and reversibly inactivating 3-MST. (C) DHLA supplementation during hyperglycemic conditions improves the function of the 3-MP/3-MST system.

Therefore, some of the conclusions and implications of the current report may also well be applicable for the pathophysiology and experimental therapy of various forms of critical illness. With respect to the therapeutic potential of the 3-MST substrate 3-MP, based on the current results, we conclude that the highest efficacy will be achieved if it is simultaneously applied with lipoic acid (and/or possibly other antioxidants).

ACKNOWLEDGMENTS

This work was supported by the American Diabetes Association (7-12-BS-184) and the National Institutes of Health (R01GM107846) to C Szabo. C Coletta was supported by a fellowship by the American Heart Association. K Módis was supported by the James W. McLaughlin Fellowship Fund of the University of Texas. The editorial assistance of Ms. Li Li Szabo is appreciated.

DISCLOSURES

The authors declare that they have no competing interests as defined by *Molecular Medicine*, or other interests that might be perceived to influence the results and discussion reported in this paper.

REFERENCES

1. Fiorucci S, Distrutti E, Cirino G, Wallace JL. (2006) The emerging roles of hydrogen sulfide in the gastrointestinal tract and liver. *Gastroenterology*. 131:259–71.
2. Szabo C. (2007) Hydrogen sulphide and its therapeutic potential. *Nat. Rev. Drug Discov*. 6:917–35.
3. Whiteman M, Winyard PG. (2011) Hydrogen sulfide and inflammation: the good, the bad, the ugly and the promising. *Expert Rev. Clin. Pharmacol*. 4:13–32.
4. Bucci M, Cirino G. (2011) Hydrogen sulphide in heart and systemic circulation. *Inflamm. Allergy Drug Targets*. 10:103–8.
5. Wang R. (2012) Physiological implications of hydrogen sulfide: a whiff exploration that blossomed. *Physiol. Rev*. 92:791–896.
6. Módis K, Wolanska K, Vozdek R. (2013) H_2S in cell signaling, signal transduction, cellular bioenergetics and physiology in C. Elegans. *Gen. Physiol. Biophys*. 32:1–22.
7. Polhemus DJ, Lefer DJ. (2014) Emergence of hydrogen sulfide as an endogenous gaseous signaling molecule in cardiovascular disease. *Circ. Res*. 114:730–7.
8. Jain SK, *et al*. (2010) Low levels of hydrogen sulfide in the blood of diabetes patients and streptozotocin-treated rats causes vascular inflammation? *Antioxid. Redox. Signal*. 12:1333–7.
9. Whiteman M, *et al*. (2010) Adiposity is a major determinant of plasma levels of the novel vasodilator hydrogen sulphide. *Diabetologia*. 53:1722–6.
10. Suzuki K, *et al*. (2011) Hydrogen sulfide replacement therapy protects the vascular endothelium in hyperglycemia by preserving mitochondrial function. *Proc. Natl. Acad. Sci. U. S. A*. 108:13829–34.
11. Ahmad FU, *et al*. (2012) Exogenous hydrogen sulfide (H_2S) reduces blood pressure and prevents the progression of diabetic nephropathy in spontaneously hypertensive rats. *Ren. Fail*. 34:203–10.
12. Xue H, *et al*. (2013) H_2S inhibits hyperglycemia-induced intrarenal renin-angiotensin system activation via attenuation of reactive oxygen species generation. *PLoS One*. 8:e74366.
13. Manna P, Jain SK. (2013) L-cysteine and hydrogen sulfide increase PIP3 and AMPK/PPARγ expression and decrease ROS and vascular inflammation markers in high glucose treated human U937 monocytes. *J. Cell. Biochem*. 114:2334–45.
14. Si YF, *et al*. (2013) Treatment with hydrogen sulfide alleviates streptozotocin-induced diabetic retinopathy in rats. *Br. J. Pharmacol*. 169:619–31.
15. Yamamoto J, *et al*. (2013) Distribution of hydrogen sulfide (H_2S)-producing enzymes and the roles of the H_2S donor sodium hydrosulfide in diabetic nephropathy. *Clin. Exp. Nephrol*. 17:32–40.
16. Wei WB, Hu X, Zhuang XD, Liao LZ, Li WD. (2014) GYY4137, a novel hydrogen sulfide-releasing molecule, likely protects against high glucose-induced cytotoxicity by activation of the AMPK/mTOR signal pathway in H9c2 cells. *Mol. Cell. Biochem*. 389:249–56.
17. Shibuya N, Mikami Y, Kimura Y, Nagahara N, Kimura H. (2009) Vascular endothelium expresses 3-mercaptopyruvate sulfurtransferase and produces hydrogen sulfide. *J. Biochem*. 146:623–6.
18. Sen U, *et al*. (2012) Increased endogenous H_2S generation by CBS, CSE, and 3MST gene therapy improves ex vivo renovascular relaxation in hyperhomocysteinemia. *Am. J. Physiol. Cell Physiol*. 303:C41–51.
19. Madden JA, Ahlf SB, Dantuma MW, Olson KR, Roerig DL. (2012) Precursors and inhibitors of hydrogen sulfide synthesis affect acute hypoxic pulmonary vasoconstriction in the intact lung. *J. Appl. Physiol. (1985)*. 112:411–8.
20. Módis K, Asimakopoulou A, Coletta C, Papapetropoulos A, Szabo C. (2013) Oxidative stress suppresses the cellular bioenergetic effect of the 3-mercaptopyruvate sulfurtransferase/hydrogen sulfide pathway. *Biochem. Biophys. Res. Commun*. 433:401–7.
21. Módis K, *et al*. (2014) Regulation of mitochondrial bioenergetic function by hydrogen sulfide. Part II. Pathophysiological and therapeutic aspects. *Br. J. Pharmacol*. 171:2123–46.
22. Hosoki R, Matsuki N, Kimura H. (1997) The possible role of hydrogen sulfide as an endogenous

smooth muscle relaxant in synergy with nitric oxide. *Biochem. Biophys. Res. Commun*. 237:527–31.
23. Zhao W, Wang R. (2002) H_2S-induced vasorelaxation and underlying cellular and molecular mechanisms. *Am. J. Physiol. Heart Circ. Physiol*. 283:H474–80.
24. Bucci M, *et al*. (2010) Hydrogen sulfide is an endogenous inhibitor of phosphodiesterase activity. *Arterioscler. Thromb. Vasc. Biol*. 30:1998–2004.
25. d'Emmanuele di Villa Bianca R, *et al*. (2011) Hydrogen sulfide-induced dual vascular effect involves arachidonic acid cascade in rat mesenteric arterial bed. *J. Pharmacol. Exp. Ther*. 337:59–64.
26. Mustafa AK, *et al*. (2011) Hydrogen sulfide as endothelium-derived hyperpolarizing factor sulfhydrates potassium channels. *Circ. Res*. 109:1259–68.
27. Coletta C, *et al*. (2012) Hydrogen sulfide and nitric oxide are mutually dependent in the regulation of angiogenesis and endothelium-dependent vasorelaxation. *Proc. Natl. Acad. Sci. U. S. A*. 109:9161–6.
28. Bucci M, *et al*. (2012) cGMP-dependent protein kinase contributes to hydrogen sulfide-stimulated vasorelaxation. *PLoS One*.7:e53319.
29. Bełtowski J, Jamroz-Wiśniewska A. (2014) Hydrogen sulfide and endothelium-dependent vasorelaxation. *Molecules* 19:21183–99.
30. Cai WJ, *et al*. (2007) The novel proangiogenic effect of hydrogen sulfide is dependent on Akt phosphorylation. *Cardiovasc. Res*. 76:29–40.
31. Papapetropoulos A, *et al*. (2009) Hydrogen sulfide is an endogenous stimulator of angiogenesis. *Proc. Natl. Acad. Sci. U. S. A*. 106:21972–7.
32. Wang MJ, *et al*. (2010) The hydrogen sulfide donor NaHS promotes angiogenesis in a rat model of hind limb ischemia. *Antioxid. Redox. Signal*. 12:1065–77.
33. Szabo C, Papapetropoulos A. (2011) Hydrogen sulphide and angiogenesis: mechanisms and applications. *Br. J. Pharmacol*. 164:853–65.
34. Polhemus DJ, *et al*. (2013) Hydrogen sulfide attenuates cardiac dysfunction after heart failure via induction of angiogenesis. *Circ. Heart Fail*. 6:1077–86.
35. Szabo C, *et al*. (2013) Tumor-derived hydrogen sulfide, produced by cystathionine-β-synthase, stimulates bioenergetics, cell proliferation, and angiogenesis in colon cancer. *Proc. Natl. Acad. Sci. U. S. A*. 110:12474–9.
36. Liu F, *et al*. (2014) Hydrogen sulfide improves wound healing via restoration of endothelial progenitor cell functions and activation of angiopoietin-1 in type 2 diabetes. *Diabetes*. 63:1763–78.
37. Goubern M, Andriamihaja M, Nübel T, Blachier F, Bouillaud F. (2007) Sulfide, the first inorganic substrate for human cells. *FASEB J*. 21:1699–706.
38. Módis K, Coletta C, Erdélyi K, Papapetropoulos A, Szabo C. (2013) Intramitochondrial hydrogen sulfide production by 3-mercaptopyruvate sulfurtransferase maintains mitochondrial electron flow and supports cellular bioenergetics. *FASEB J*. 27:601–11.
39. Módis K, Panopoulos P, Coletta C, Papapetropoulos A, Szabo C. (2013) Hydrogen sulfide-mediated stimulation of mitochondrial electron transport involves inhibition of the mitochondrial phosphodiesterase 2A, elevation of cAMP and activation of protein kinase A. *Biochem. Pharmacol*. 86:1311–9.
40. Szczesny B, *et al*. (2014) AP39, a novel mitochondria-targeted hydrogen sulfide donor, stimulates cellular bioenergetics, exerts cytoprotective effects and protects against the loss of mitochondrial DNA integrity in oxidatively stressed endothelial cells in vitro. *Nitric Oxide*.41:120–30.
41. Helmy N, *et al*. (2014) Oxidation of hydrogen sulfide by human liver mitochondria. *Nitric Oxide*. 41:105–12.
42. Szabo C, *et al*. (2014) Regulation of mitochondrial bioenergetic function by hydrogen sulfide. Part I. Biochemical and physiological mechanisms. *Br. J. Pharmacol*. 171:2099–122.
43. Mikami Y, *et al*. (2011) Thioredoxin and dihydrolipoic acid are required for 3-mercaptopyruvate sulfurtransferase to produce hydrogen sulfide. *Biochem. J*. 439:479–85.
44. Cameron NE, Jack AM, Cotter MA. (2001) Effect of alpha-lipoic acid on vascular responses and nociception in diabetic rats. *Free Radic. Biol. Med*. 31:125–35.
45. Nebbioso M, Pranno F, Pescosolido N. (2013) Lipoic acid in animal models and clinical use in diabetic retinopathy. *Expert Opin. Pharmacother*. 14:1829–38.
46. Committee for the Update of the Guide for the Care and Use of Laboratory Animals, Institute for Laboratory Animal Research, Division on Earth and Life Studies, National Research Council of the National Academies. (2011) *Guide for the Care and Use of Laboratory Animals*. 8th edition. Washington (DC): National Academies Press.
47. Warner TD. (1990) Simultaneous perfusion of rat isolated superior mesenteric arterial and venous beds: comparison of their vasoconstrictor and vasodilator responses to agonists. *Br. J. Pharmacol*. 99:427–33.
48. Ferreira FM, Palmeira CM, Seiça R, Moreno AJ, Santos MS. (2003) *Diabetes* and mitochondrial bioenergetics: alterations with age. *J. Biochem. Mol. Toxicol*. 17:214–22.
49. Szabo C. (2009) Role of nitrosative stress in the pathogenesis of diabetic vascular dysfunction. *Br. J. Pharmacol*. 156:713–27.
50. Sivitz WI, Yorek MA. (2010) Mitochondrial dysfunction in diabetes: from molecular mechanisms to functional significance and therapeutic opportunities. *Antioxid. Redox. Signal*. 12:537–77.
51. Giacco F, Brownlee M. (2010) Oxidative stress and diabetic complications. *Circ. Res*. 107:1058–70.
52. Papanas N, Ziegler D. (2014) Efficacy of α-lipoic acid in diabetic neuropathy. *Expert Opin. Pharmacother*. 15:2721–31.
53. Nebbioso M, Pranno F, Pescosolido N. (2013) Lipoic acid in animal models and clinical use in diabetic retinopathy. *Expert Opin. Pharmacother*. 14:1829–38.
54. Kiguchi S. (1983) Metabolism of 3-mercaptopyruvate in rat tissues. *Acta Med. Okayama*. 37:85–91.
55. Shibuya N, *et al*. (2009) 3-Mercaptopyruvate sulfurtransferase produces hydrogen sulfide and bound sulfane sulfur in the brain. *Antioxid. Redox. Signal*. 11:703–14.
56. Nagahara N, Katayama A. (2005) Post-translational regulation of mercaptopyruvate sulfurtransferase via a low redox potential cysteine-sulfenate in the maintenance of redox homeostasis. *J. Biol. Chem*. 280:34569–76.
57. Miyamoto R, Otsuguro K, Yamaguchi S, Ito S. (2014) Contribution of cysteine aminotransferase and mercaptopyruvate sulfurtransferase to hydrogen sulfide production in peripheral neurons. *J. Neurochem*. 130:29–40.
58. Nagahara N, Nirasawa T, Yoshii T, Niimura Y. (2012) Is novel signal transducer sulfur oxide involved in the redox cycle of persulfide at the catalytic site cysteine in a stable reaction intermediate of mercaptopyruvate sulfurtransferase? *Antioxid. Redox. Signal*. 16:747–53.
59. Nagahara N. (2013) Regulation of mercaptopyruvate sulfurtransferase activity via intrasubunit and intersubunit redox-sensing switches. *Antioxid. Redox. Signal*. 19:1792–802.
60. Yadav PK, Yamada K, Chiku T, Koutmos M, Banerjee R. (2013) Structure and kinetic analysis of H_2S production by human mercaptopyruvate sulfurtransferase. *J. Biol. Chem*. 288:20002–13.
61. Flannigan KL, Ferraz JG, Wang R, Wallace JL. (2013) Enhanced synthesis and diminished degradation of hydrogen sulfide in experimental colitis: a site-specific, pro-resolution mechanism. *PLoS One*. 8:e71962.
62. Nie LH, *et al*. (2013) Effects of intrauterine cigarette smoking exposure on expression of 3-mercaptopyruvate sulfurtransferase in medulla oblongata of neonatal rats [in Chinese]. *Sichuan Da Xue Xue Bao Yi Xue Ban*. 44:526–30.
63. Li M, *et al*. (2013) Chronic intermittent hypoxia promotes expression of 3-mercaptopyruvate sulfurtransferase in adult rat medulla oblongata. *Auton. Neurosci*. 179:84–9.
64. Zhao H, Chan SJ, Ng YK, Wong PT. (2013) Brain 3-mercaptopyruvate sulfurtransferase (3MST): cellular localization and downregulation after acute stroke. *PLoS One*. 8:e67322.
65. Nagahara N, *et al*. (2013) Antioxidant enzyme, 3-mercaptopyruvate sulfurtransferase-knockout mice exhibit increased anxiety-like behaviors: a model for human mercaptolactate-cysteine disulfiduria. *Sci. Rep*. 3:1986.
66. Yusuf M, *et al*. (2005) Streptozotocin-induced diabetes in the rat is associated with enhanced tissue hydrogen sulfide biosynthesis. *Biochem. Biophys. Res. Commun*. 333:1146–52.
67. Szabo C. (2012) Roles of hydrogen sulfide in the pathogenesis of diabetes mellitus and its complications. *Antioxid. Redox. Signal*. 17:68–80.
68. Langouche L, Mesotten D, Vanhorebeek I. (2010) Endocrine and metabolic disturbances in critical illness: relation to mechanisms of organ dysfunction and adverse outcome. *Verh. K. Acad Geneeskd. Belg*. 72:149–63.
69. Rizk M, Witte M, Barbul A. (2004) Nitric oxide and wound healing. *World J. Surg*. 28:301–6.
70. Buganza Tepole A, Kuhl E. (2013) Systems-based approaches toward wound healing. *Pediatr Res*. 73:553–63.

Cite this article as: Coletta C, *et al.* (2015) Regulation of vascular tone, angiogenesis and cellular bioenergetics by the 3-mercaptopyruvate sulfurtransferase/H_2S pathway: functional impairment by hyperglycemia and restoration by DL-α-lipoic acid. *Mol. Med*. 21:1–14.